

# Constrained Kalman Filtering for Indoor Localization of Transport Vehicles Using Floor-Installed HF RFID Transponders

Christof Röhrig, Daniel Heß, Frank Künemund  
University of Applied Sciences and Arts in Dortmund  
Intelligent Mobile Systems Lab, Otto-Hahn-Str. 23, 44227 Dortmund, Germany  
Web: [www.ims1.fh-dortmund.de](http://www.ims1.fh-dortmund.de), Email: [roehrig@ieee.org](mailto:roehrig@ieee.org)

**Abstract**—Localization of transport vehicles is an important issue for many intralogistics applications. The paper presents an inexpensive solution for indoor localization of vehicles. Global localization is realized by detection of RFID transponders, which are integrated in the floor. The paper presents a novel algorithm for fusing RFID readings with odometry using Constraint Kalman filtering. The paper presents experimental results with a Mecanum based omnidirectional vehicle on a NaviFloor® installation, which includes passive HF RFID transponders. The experiments show that the proposed Constraint Kalman filter provides a similar localization accuracy compared to a Particle filter but with much lower computational expense.

## I. INTRODUCTION

Changing requirements in industrial production and transportation systems demand flexible material handling systems [1]. Shorter product life-cycles, mass customization, and stricter quality requirements lead to a higher complexity in logistics processes. These challenges may be alleviated by technologies like new material handling systems and RFID technology [2]. Flexible material handling can be addressed by using small autonomous transport vehicles, which act as a swarm of mobile robots. Several companies have introduced small robotic vehicles for intralogistic applications. Examples are the “Kiva automated material handling system”, “ADAM™ (Autonomous Delivery and Manipulation)”, Grenzebach G-Pro and Adept Courier. Furthermore, in several research projects small low cost vehicles are developed. Examples are “KARIS Kleinskaliges Autonomes Redundantes Intralogistik System”, KaTe “Kleine autonome Transporteinheiten” and LOCATIVE “Low Cost Automated Guided Vehicle” [3].

Inexpensive localization of small robotic vehicles is an important issue for many intralogistic applications and object of current research activities. A solution for low cost localization is the dual use of technologies, which are needed for the operation of the vehicles. One example is the usage of IEEE 802.15.4 CSS for communication as well as for global localization and laser range finders for safety as well as for detecting landmarks and local localization [4].

In several low cost low weight robotic vehicles, safety laser range finders are not implemented, because of their relatively high cost. A possible solution for global localization is the



Figure 1. Structure of the NaviFloor®

usage of auto-ID technology as artificial landmarks. Kiva uses 2D bar codes on the floor, which can be detected with a camera by the vehicles [5]. These bar codes specify the pathways and guarantee accurate localization. Drawbacks of this solution are the risk of polluting the bar codes and the need for predefined pathways, which restrict the movements of the vehicles.

Another possible solution for global localization is the usage of RFID technology as artificial landmarks. Passive RFID technology is often used in logistics and warehouse management for object identification and tracking. Typically the field of application is defined by the detection range of the RFID transponders, which depends on the operation frequency. Usually LF or HF technology is used for self-localization of mobile systems (reader localization) and UHF technology is used for object identification in logistics applications [6] and service robotics [7].

The basic idea of using passive RFID transponders as artificial landmarks for self-localization of mobile systems is not new. LF RFID transponders are used to mark a predefined pathway for navigation of Automated Guided Vehicles (AGVs) in industry since more than two decades [8]. For this purpose, transponders are buried in the ground along the pathway of the vehicles. LF transponders can be detected by RFID readers, which are attached at the vehicles. Detected transponder are compared with a map that contains serial numbers of RFID transponders along with their corresponding positions. The control system of the AGV interpolates a trajectory to the next transponder on the pathway and controls steering and speed.

This work was supported in part by the Federal Ministry of Economics and Energy of the German State (ZIM, grant number KF2795209).

Odometry using wheel encoders is needed to move from one transponder to the next one.

A known disadvantage of using LF RFID transponders for vehicle navigation is the speed limitation of the vehicles caused by the low data transfer rate of LF transponders. Also LF transponders are comparatively expensive and the ground must be prepared with holes for these transponders [9]. Owing to the cost of installation and material, the transponders are installed on the pathway of the vehicles only.

An inexpensive and much more flexible option is the usage of a grid of floor installed standard HF RFID transponders. This allows free navigation of vehicles without the need of predefined pathways. The cost of a passive transponder is less than 0.2€. A commercially available product, which employs passive HF RFID transponders in a floor is the NaviFloor<sup>®</sup> manufactured by Future-Shape (see Fig. 1). Technical details of the NaviFloor<sup>®</sup> can be found in Sec. V-A.

This paper extends the work we have presented in [10]. The main contribution of this paper is the development of a novel localization algorithm, which fuses the information from RFID readings with odometry using Constrained Kalman filtering. Only an inexpensive HF RFID reader and wheel encoders are needed for the proposed localization algorithm. The proposed algorithm requires a RFID reader with the capability of detecting transponders only, no additional sensory information such as RSSI is required. The localization accuracy of the proposed algorithm is comparable to the accuracy of a Particle filter (Sequential Monte Carlo method), but requires less computations. Furthermore in this paper, we compare our localization algorithm based on Constrained Kalman filtering with the Quantized Kalman filter we have developed in [10]. Our experimental results show that the Constrained Kalman filter provides a better accuracy compared to the Quantized Kalman filter while needing a similar computational effort. The proposed algorithm can be implemented in the measurement update of any nonlinear Kalman filter.

The rest of the paper is organized as follows: In Sec. II the localization problem using floor installed RFID transponders is defined. Sec. III presents related work. The proposed localization algorithm based on Constrained Kalman filtering is developed in Sec. IV. In Sec. V the experimental setup including transport vehicle and NaviFloor<sup>®</sup> is described. Experimental results are presented in Sec. VI. Finally, the conclusions are given in Sec. VII.

## II. PROBLEM FORMULATION

We consider the problem of global localizing a vehicle in a known environment. In this context, global localization means that the initial pose of the vehicle is not known a priori. The vehicle is equipped with a RFID reader and moves over a floor with  $n$  RFID transponders. The position of the transponders is known a priori. The vehicle moves in 2D space, the pose of the vehicle (position and heading) in the world frame is defined as  $\mathbf{x} = (x, y, \theta)^T$  in the configuration space (C-space)  $\mathcal{C}$ , which is a subset of  $\mathbb{R}^3$ .  $\mathcal{C} = \mathbb{R}^2 \times \mathcal{S}^1$  takes into account that  $\theta \pm 2\pi$  yields to equivalent headings ( $\theta \in [0, 2\pi)$ ). If a transponder  $T_i \in \{T_1, \dots, T_n\}$  with position  $\mathbf{t}_i = (x_i, y_i)^T$  (defined in the world frame) is in range of the reader antenna, it is detected by the vehicle. The area where a transponder can be detected by

the reader is the detection area  $\mathcal{A}$ . The detection area can be described in the antenna frame, which is in a fixed position in the vehicle frame. Size and shape of  $\mathcal{A}$  depend on the reader antenna, the transponder type and the distance between them and is the same for all transponders. The position of a tag in the antenna frame  $\mathbf{z}_i = ({}^A x_i, {}^A y_i)^T$  can be described by

$$\mathbf{z}_i = \mathbf{h}(\mathbf{x}, \mathbf{t}_i), \quad (1)$$

where  $\mathbf{x}$  is the pose of the vehicle and  $\mathbf{t}_i$  is the position of the tag  $T_i$ , both defined in the world frame.

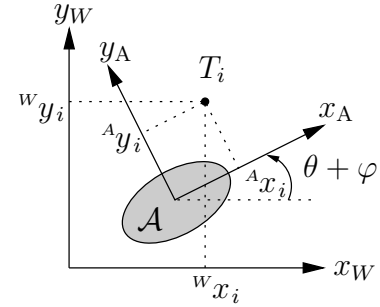


Figure 2. Position of RFID tag in world frame  $({}^W x_i, {}^W y_i)^T$  and in antenna frame  $({}^A x_i, {}^A y_i)^T$ . The detection area  $\mathcal{A}$  is marked in gray.

Fig. 2 shows the position of a RFID tag in the world frame and in the antenna frame. The rotation angle between the antenna frame and the world frame depends on the heading of the vehicle ( $\theta$ ) and the constant alignment of the antenna ( $\varphi$ ) with respect to the vehicle frame.

$\mathbf{h}(\cdot)$  can be defined by a homogeneous transformation in 2D:

$$\tilde{\mathbf{z}} = {}^A \mathbf{T}_W(\mathbf{x}) \cdot \tilde{\mathbf{t}}, \quad (2)$$

where the transformation matrix

$${}^A \mathbf{T}_W(\mathbf{x}) = {}^A \mathbf{T}_V \cdot {}^V \mathbf{T}_W(\mathbf{x})$$

consists of the constant transformation from vehicle frame into antenna frame  ${}^A \mathbf{T}_V = \mathbf{f}(x_A, y_A, \varphi)$  and the transformation from world frame into vehicle frame  ${}^V \mathbf{T}_W$ , which depends on the pose of the vehicle  ${}^V \mathbf{T}_W = \mathbf{f}(\mathbf{x})$  with  $\mathbf{x} = (x, y, \theta)^T$ :

$${}^V \mathbf{T}_W = \begin{pmatrix} \cos \theta & \sin \theta & -x \cos \theta - y \sin \theta \\ -\sin \theta & \cos \theta & x \sin \theta - y \cos \theta \\ 0 & 0 & 1 \end{pmatrix},$$

$${}^A \mathbf{T}_V = \begin{pmatrix} \cos \varphi & \sin \varphi & -x_A \cos \varphi - y_A \sin \varphi \\ -\sin \varphi & \cos \varphi & x_A \sin \varphi - y_A \cos \varphi \\ 0 & 0 & 1 \end{pmatrix},$$

$\tilde{\mathbf{z}}$  and  $\tilde{\mathbf{t}}$  are homogeneous coordinates in 2D  $(x, y, 1)^T$ . The probability of detecting a transponder  $T_i$  at a position  $\mathbf{z}_i = ({}^A x_i, {}^A y_i)^T$  inside the detection area  $\mathcal{A}$  of the reader is nearly 1 and outside the area it is zero:

$$p(T_i | \mathbf{z}_i) \begin{cases} 1 & \text{if } \mathbf{z}_i \in \mathcal{A} \\ 0 & \text{else} \end{cases} \quad (3)$$

False positive readings do not arise, owing to the short range of HF RFID technology. Therefore, the RFID reader can be treated as a binary detector if  $\mathbf{z}_i \in \mathcal{A}$  or not. All positions  $\mathbf{z}_i$  that fall in the detection area  $\mathcal{A}$  of the reader lead to the same measurement.

Bayesian filtering is a solution for estimating the pose of a vehicle using RFID readings and odometry. Aim of the pose estimation using RFID readings is to obtain the probability density  $p(\mathbf{x}_k|T_i, \mathbf{x}_{k-1}, \mathbf{u}_k) = p(\mathbf{x}_k|z_i \in \mathcal{A}, \mathbf{x}_{k-1}, \mathbf{u}_k)$ , where  $\mathbf{u}_k$  is the odometry of the vehicle obtained from wheel encoders. This can be achieved by applying a Bayesian filter:

$$p(\mathbf{x}_k|z_i \in \mathcal{A}, \mathbf{x}_{k-1}, \mathbf{u}_k) = \frac{p(z_i \in \mathcal{A}|\mathbf{x}_k)p(\mathbf{x}_k|\mathbf{x}_{k-1}, \mathbf{u}_k)}{p(z_i \in \mathcal{A})} \quad (4)$$

where  $p(z_i \in \mathcal{A}|\mathbf{x}_k)$  is the probability of measuring  $T_i$  at the pose  $\mathbf{x}$  in time step  $k$  and  $p(\mathbf{x}_k|\mathbf{x}_{k-1}, \mathbf{u}_k)$  is the motion model of the vehicle. Due to the highly non-Gaussian probability distribution of RFID transponder readings, usually Particle Filters (PF) are used for this purpose. In a PF, the probability density of the pose estimate is approximated by a set of particles. Every particle in the set represents a weighted hypothesis of the pose  $\mathbf{x}$ . This enables the filter to handle non-Gaussian and multimodal distributions. After a tag is detected, every particle in the set is distributed through function (1) and weighted with probability (3). Main drawback of the PF is the computational expense associated with it, because only large particle counts lead to good pose estimates. Thus, there is some effort to replace the PF with methods based on Kalman filtering.

A RFID measurement can be interpreted as a *quantized measurement* of a position, which may depend on the headings of the vehicle. The quantization depends on the size of  $\mathcal{A}$  and can be modeled by quantization noise. This interpretation leads to a localization algorithm, which is based on Quantized Kalman filtering [10]. In order to reduce the number of transponders needed in the grid, the size of the grid and therefore the detection area has to be relatively large. If the detection area compared to the grid size is small, the chance of detecting a transponders while traveling over the grid decreases, which reduces the localization accuracy. Main drawback of Quantized Kalman filtering is the large quantization noise for large detection areas, which leads to low estimation accuracy.

A different interpretation of a RFID measurement  $T_i$  is that the pose of the vehicle falls in a *constrained region* in the C-space  $\mathcal{C}$ . This detection region  $\mathcal{R}_i \subset \mathcal{C}$  is defined by the position of the tag  $t_i = (x, y)^T$  in the world frame, the placement of the antenna with respect to the vehicle frame  ${}^A T_W$  and the shape of the detection area  $\mathcal{A}$  in the antenna frame. The detection region  $\mathcal{R}_i$  can be interpreted as an extension of the 2D detection area  $\mathcal{A}$  to the 3D C-space of the vehicle. This means that the position of the vehicle falls in a bounded area, which depends on the heading of the vehicle. Based on this interpretation, we develop a novel localization algorithm based on Constrained Kalman filtering in this paper.

### III. RELATED WORKS

In order to allow free navigation of robotic vehicles, some research on RFID localization using a grid of floor-installed RFID tags has been done. Kodaka et al. apply a PF for pose estimation of a mobile robot using floor based RFID transponder and odometry [11]. As mentioned above, main drawback of the PF is the computational expense associated with it. Thus, there is some effort to replace the PF with methods based on Kalman filtering. Choi et al. propose the fusion of ultrasonic sensors, odometry and readings of HF RFID transponders, which are

integrated in the floor [12]. This localization algorithm is based on Kalman filtering but needs additional sensors and mapping of the environment. Lee et al. have developed a Gaussian measurement model for UHF RFID transponders embedded in the floor, which is suitable for Kalman filtering [13]. Its application in a Kalman filter has less computational expense but provides not the same localization accuracy as a PF.

There is also some research on UHF tags at walls or ceilings for self-localization of robotic vehicles. DiGiampaolo and Martinelli have developed a Quantized Extended Kalman Filter algorithm for localization on mobile robots using UHF RFID tags at the ceiling [14]. Boccadoro et. al. propose a Constrained Kalman filter for global localization of mobile robots using UHF RFID technology and odometry [15]. In that research, the transponders are placed at the walls in an indoor environment. As in this paper, their proposed algorithm is based on Constraint Kalman filtering. Since wall placed UHF transponders provide a different detection behavior than floor placed HF transponders, their localization algorithm is completely different to the algorithm proposed in this paper and is based on numerical histogram filtering. Levratti et. al. present a localization algorithm for robotic lawnmowers based on the Constrained Kalman filter proposed in [15]. It merges odometry with UHF RFID transponders, which are placed at the borders of the working area [16].

The usage of HF transponders in the floor for self-localization has some advantages over usage of long range UHF technology at the walls or the ceiling. Usually the detection area is smaller and therefore the localization accuracy is better compared to long range UHF technology. HF RFID technology behaves different from long range UHF RFID technology, that is investigated in the research mentioned above, and therefore needs different modeling. In particular, floor placed HF RFID transponders have a nearly binary detection characteristic, where the detection area depends mainly on size and shape of the reader's antenna.

## IV. PROPOSED LOCALIZATION ALGORITHMS

This section describes the pose estimation in three different types of Bayesian filters. A Bayesian filter for vehicle localization needs a motion model of the vehicle and a sensor model of its measurements. The proposed algorithm is independent of the motion model. For experimental evaluation, we use an omnidirectional vehicle with Mecanum wheels. The motion model of this vehicle is described in Sec. V-C. In this section, the sensor model of RFID readings and the proposed algorithm for measurement update of the Bayesian filters are described. As mentioned before, usually PFs are deployed in RFID localization algorithms, because of the highly nonlinear and quantized measurements by the RFID reader. A PF will be used as benchmark for our proposed localization algorithm based on Constrained Kalman filtering. A Quantized Kalman filter serves as a second benchmark.

### A. Constrained Kalman Filtering

A RFID measurement gives the information if a transponder  $T_i$  with the position  $t_i$  is inside or outside the detection area  $\mathcal{A}$  of the reader. Beside this binary nature of RFID measurements there are additional sources of uncertainty:

- Communication delay between the RFID reader and the transponder: This delay is caused by the limited data rate of the air interface and the collision avoidance procedure for multi tag readings.
- Communication delay between the control system and the RFID reader: This delay is caused by the processing time of the reader and the limited data rate on the interface to the reader.
- Variations in tag placement: Due to production tolerances and manual placement, the position of the RFID tags may differ from the regular grid.

The uncertainty in the tag placement can be treated as Gaussian noise. The communication delays causes additional noise that depends on the speed of the vehicle.

With this additional uncertainty, the measurement function (1) can be extended:

$$z_i = \mathbf{h}(\mathbf{x}, \mathbf{t}_i, \mathbf{v}), \quad (5)$$

where  $\mathbf{v}$  is the measurement noise caused by communication delays and tag misplacement due to production tolerances. We assume that  $\mathbf{v}$  is normally distributed with zero mean.

When the RFID tag  $T_i$  is detected, the position  $z_i$  must be inside the detection area  $\mathcal{A}$ . This implies, that the pose of the vehicle must be inside the detection region  $\mathbf{x} \in \mathcal{R}_i$ , with  $\mathcal{R}_i \subset \mathcal{C}$ . The detection region  $\mathcal{R}_i$  is defined by the position of the tag  $\mathbf{t}_i = (x, y)^T$  in the world frame, the placement of the antenna with respect to the vehicle frame and the shape of the detection area  $\mathcal{A}$  in the antenna frame (see Sec. II). This information can be interpreted as a noisy nonlinear state inequality constraint [17].

In order to define the state constraints of the vehicle, we define a nonlinear function

$$d_i = g(z_i) \quad (6)$$

that describes the distance of the transponder to the border of  $\mathcal{A}$ , where

$$g(z_i) \begin{cases} \leq 0 & \text{if } z_i \in \mathcal{A} \\ > 0 & \text{else} \end{cases} \quad (7)$$

A nonlinear state inequality constraint can be transformed into a nonlinear state equality constraint [18], since two cases can occur:

- 1) The inequality is satisfied and so do not have to be taken into account.
- 2) The inequality is not satisfied. Then, the equality constraint has to be applied.

Owing to the uncertainty in RFID measurements, we treat the (soft) equality constraint as a noisy measurement:

$$g(z_i) = g(\mathbf{h}(\mathbf{x}, \mathbf{t}_i, \mathbf{v})) = 0 \quad (8)$$

- 1) If the inequality constraint (7) is satisfied, no measurement update of the Kalman filter is applied.
- 2) If a transponder  $T_i$  is detected but  $g(\hat{z}_i) > 0$ , then we apply a measurement update  $g(\hat{z}_i) = 0$  in every time step  $k$  until the constraint is satisfied.
- 3) If the transponder is not longer detected, but the pose estimate persists in  $\mathcal{R}_i$ , which means that

$g(\mathbf{h}(\hat{\mathbf{x}}_k, \mathbf{t}_i, \mathbf{0})) < 0$ , then we apply a measurement update  $g(\hat{\mathbf{x}}_k) = 0$  again in every time step  $k$  until the constraint is satisfied.

Every measurement update moves the pose estimate in direction of the border of  $\mathcal{R}_i$ . This algorithm is applicable for any RFID equipment, where the border of the detection area can be described by a nonlinear function (8). If more than one transponder can be detected at a moment, the constraints of all detected transponders have to be considered simultaneously. The described algorithm can be applied to any nonlinear Kalman filter, e.g. the well known Extended Kalman Filter (EKF).

The application of the proposed algorithm to the measurement update of an EKF leads to

$$\begin{aligned} \mathbf{K}_k &= \mathbf{P}_k \mathbf{G}_k^T (\mathbf{G}_k \mathbf{P}_k \mathbf{G}_k^T + \mathbf{V}_k \mathbf{R}_k \mathbf{V}_k^T)^{-1} \\ \hat{\mathbf{x}}_k^+ &= \hat{\mathbf{x}}_k - \mathbf{K}_k g(\mathbf{h}(\hat{\mathbf{x}}_k, \mathbf{t}_i, \mathbf{0})) \\ \mathbf{P}_k^+ &= (\mathbf{I} - \mathbf{K}_k \mathbf{G}_k) \mathbf{P}_k \end{aligned} \quad (9)$$

where  $\mathbf{K}_k$  is the Kalman gain,  $\hat{\mathbf{x}}_k^+$  and  $\mathbf{P}_k^+$  are the estimated pose and its covariance after the RFID measurement update,  $\mathbf{G}_k = \frac{\partial g}{\partial \mathbf{x}}(\hat{\mathbf{x}}_k, \mathbf{t}_i, \mathbf{0})$ ,  $\mathbf{V}_k = \frac{\partial g}{\partial \mathbf{v}}(\hat{\mathbf{x}}_k, \mathbf{t}_i, \mathbf{0})$  and  $\mathbf{R}_k$  is the covariance matrix of the uncertainty  $\mathbf{v}_k \sim \mathcal{N}(\mathbf{0}, \mathbf{R}_k)$ .

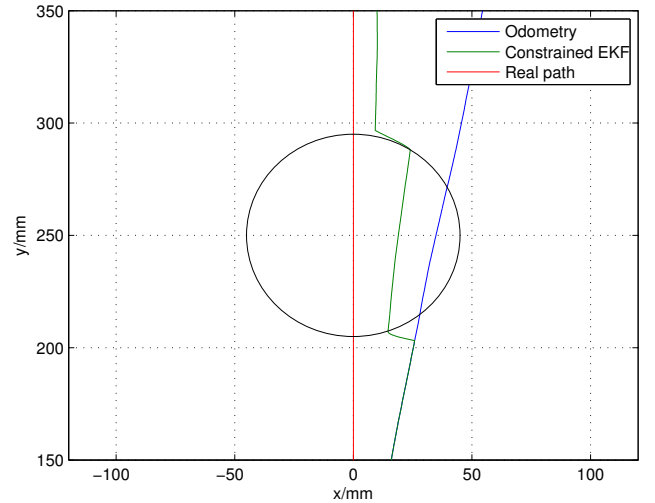


Figure 3. Visualization of Constrained EKF

Fig. 3 shows results from a simulation and demonstrates the working principal of the Constrained Kalman filtering. For simplification it is assumed that the reader antenna is mounted in the center of the vehicles frame ( ${}^A T_V = \mathbf{I}$ ). The detection area  $\mathcal{A}$  can be described by a circle with radius  $r = 45$  mm (see Sec. VI). In this case, the detection region  $\mathcal{R}_i$  of the tag  $T_i$  has a cylindrical shape in the state space of the vehicle. The projection of  $\mathcal{R}_i$  onto the 2D working area is a circle with radius  $r$  and center at  $\mathbf{t}_i$ .

The vehicle moves from position  $(0, 0)$  in  $y$  direction with  $\dot{y} = 100$  mm/s. The sample time for the motion update (odometry) is  $T = 3$  ms, the update time of the RFID reader is  $T_{\text{RFID}} = 21$  ms. The pose estimated by odometry is corrupted by noise and is shown as blue curve. The real trajectory is shown in red, the estimate in green. A RFID tag  $T_1$  is placed at  $x_1 = 0$  mm,  $y_1 = 250$  mm. After the tag  $T_1$  is detected, the constraint  $g(\mathbf{h}(\hat{\mathbf{x}}_k, \mathbf{t}_1, \mathbf{0})) \leq 0$  is checked. Since the constraint

is not satisfied, a measurement update is applied, which moves the pose estimate to the border of  $\mathcal{R}_1$ . This update is repeated in every time step  $k$  until the constraint is satisfied. If the constraint is satisfied, while the vehicle is moving through the detection region, no measurement updates are applied. After the estimated pose leaves  $\mathcal{R}_1$ , measurement updates are applied in every time step  $k$  until the tag is not longer detected. This moves the estimated pose  $\hat{\mathbf{x}}_k$  in direction of the border of  $\mathcal{R}_1$  again. The correction of  $\hat{\mathbf{x}}_k$  depends on its covariance matrix  $\mathbf{P}_k$  and the shape of  $\mathcal{A}$ . Thus, there is a small remaining pose error in x direction.

### B. Quantized Kalman Filtering

In this section, the Quantized Kalman filter we have proposed in [10] is adapted to a different definition of the measurement function (5). The detection of a transponder can be considered as a quantized measurement of a position. The center of the detection area  $\mathcal{A}$  defines the position measurement in the antenna frame. The size of  $\mathcal{A}$  is a measure of the uncertainty in the measurement and can be modeled as quantization noise. After detecting the transponder  $T_i$ , the predicted measurement is defined by  $\hat{z}_i = \mathbf{h}(\hat{\mathbf{x}}_k, \mathbf{t}_i, \mathbf{0})$ .

The *Gaussian-Fit Algorithm* proposed by Curry [19, p. 23–25] is applied to nonlinear Kalman filtering. The first and second moment of  $p(\mathbf{z}_i | \mathbf{z}_i \in \mathcal{A})$  are needed in the measurement update of a nonlinear KF. For notational convenience let

$$\boldsymbol{\mu} = \mathbb{E}(\mathbf{z}_i | \mathbf{z}_i \in \mathcal{A}), \quad \boldsymbol{\Sigma} = \text{cov}(\mathbf{z}_i | \mathbf{z}_i \in \mathcal{A}).$$

Mean  $\boldsymbol{\mu}$  and covariance  $\boldsymbol{\Sigma}$  of the detection area  $\mathcal{A}$  can be calculated in advance using numerical integration (see [10]). Additional measurement noise caused by communication delays and tag misplacement due to production tolerances can be modeled with a random variable  $\mathbf{v}_k$ . It is assumed that  $\mathbf{v}_k \sim \mathcal{N}(\mathbf{0}, \mathbf{R}_k)$ .

Before the measurement update is performed, the innovation of the measurement  $T_i$  is checked. If  $\hat{z}_i = \mathbf{h}(\hat{\mathbf{x}}_k, \mathbf{t}_i, \mathbf{0}) \in \mathcal{A}$ , the detection of  $T_i$  is predicted and the innovation is zero (the detection of  $T_i$  gives no additional information). Thus, no measurement update is performed. The measurement update is performed only, if  $\hat{z}_i \notin \mathcal{A}$ . Every measurement update moves the pose estimate in direction of the center of  $\mathcal{R}_i$ . The described algorithm can be applied to the measurement update of any nonlinear Kalman filter. The application of the standard EKF algorithm leads to:

$$\mathbf{K}_k = \mathbf{P}_k \mathbf{H}_k^T (\mathbf{H}_k \mathbf{P}_k \mathbf{H}_k^T + \mathbf{V}_k (\mathbf{R}_k + \boldsymbol{\Sigma}) \mathbf{V}_k^T)^{-1} \quad (10)$$

$$\hat{\mathbf{x}}_k^+ = \hat{\mathbf{x}}_k + \mathbf{K}_k (\boldsymbol{\mu} - \mathbf{h}(\hat{\mathbf{x}}_k, \mathbf{t}_i, \mathbf{0})) \quad (11)$$

$$\mathbf{P}_k^+ = (\mathbf{I} - \mathbf{K}_k \mathbf{H}_k) \mathbf{P}_k \quad (12)$$

where  $\mathbf{H}_k = \frac{\partial \mathbf{h}}{\partial \mathbf{x}}(\hat{\mathbf{x}}_k, \mathbf{t}_i, \mathbf{0})$  and  $\mathbf{V}_k = \frac{\partial \mathbf{h}}{\partial \mathbf{v}}(\hat{\mathbf{x}}_k, \mathbf{t}_i, \mathbf{0})$ .

### C. Particle Filter

As mentioned before, usually PFs are deployed in RFID localization algorithms, because of the highly nonlinear and quantized measurements by the RFID reader. A PF will be used as benchmark for our proposed localization algorithm based on Constrained Kalman filtering.

In the motion update of a PF, all particles are sampled with a random generator and distributed through the motion

model of the vehicle. The measurement update in a particle filter is straight forward (see also [11]). After the vehicle has detected a RFID transponder, each particle  $\mathbf{x}_k^j$  is distributed through the measurement function  $\mathbf{z}_i^j = \mathbf{h}(\mathbf{x}_k^j, \mathbf{t}_i, \mathbf{0})$  and then weighted with the associated probability ( $w_j = p(T_i | \mathbf{z}_i^j)$ ). The measurement noise can be modeled with a normal distribution  $\mathbf{v}_k \sim \mathcal{N}(\mathbf{0}, \mathbf{R}_k)$ .

If no particle falls inside the detection area ( $\sum w_j \approx 0$ ), the particle set has to be reinitialized. In this case, the particles are uniformly distributed in the detection region  $\mathcal{R}_i$ . Otherwise, the particle set is normalized and resampled.

### D. Global Localization

A Kalman filter has to be initialized with a rough initial pose estimate of the vehicle. Since a RFID reading provides no information about the heading of the vehicle, at least two different RFID transponders have to be detected to initialize a Kalman filter. This initial procedure is a kind of map-matching between the initial local map of the vehicle processed by odometry and the global map including the positions of the transponders. The heading can be estimated after detecting two different RFID transponders ( $T_i, T_j$ ):

$$\hat{\theta}_k = \theta_k^1 + \text{atan2}(\Delta y, \Delta x) - \text{atan2}(\Delta y^1, \Delta x^1), \quad (13)$$

where  $\theta_k^1$  is the local heading while detecting the second transponder,  $\Delta x = x_j - x_i$ ,  $\Delta y = y_j - y_i$  are the distances between the detected transponders and  $\Delta y^1, \Delta x^1$  are the distances of the trajectory traveled in the local map.  $\theta_k^1$  has to be considered, because an omnidirectional vehicle can move in any direction without changing its heading. The estimation of  $\hat{\theta}_k$  is very rough, because  $\Delta x, \Delta y$  are quantized with the grid size of the RFID transponders.

## V. EXPERIMENTAL SETUP

### A. NaviFloor<sup>®</sup>

The NaviFloor<sup>®</sup> is a glass fiber reinforcement in which passive HF RFID transponders are embedded. The NaviFloor<sup>®</sup> underlay is shipped in rolls including a map of the RFID transponders for simplification of the installation [20]. The NaviFloor<sup>®</sup> is specially developed for installation beneath artificial flooring (see Fig. 1). It is pressure-resistant up to 45 N/mm<sup>2</sup> and withstands even heavy indoor vehicles like fork lift trucks.

We have installed a NaviFloor<sup>®</sup> in our robotics lab. Fig. 4 shows a picture taken during the installation procedure. The RFID transponders are installed in a grid of 25 cm. The whole installation includes nearly thousand RFID transponders. The transponders embedded in the NaviFloor<sup>®</sup> have a rectangular shape 45 mm × 45 mm. NXP chips I-CODE SLI are integrated in the transponders. The transponders are compliant to ISO 15693 and communicate in the 13.56 MHz HF band.

### B. RFID Readers

We use two different RFID readers for our experiments. The first reader is a ‘‘SkyeModule M1’’ (*reader 1*). The HF antenna of this reader has a rectangular shape with the dimension of 38 mm × 40 mm. A transponder is detected, if the antennas



Figure 4. NaviFloor® Installation in our robotics lab

of transponder and reader have a small overlap. The detection range between reader and antenna at maximum overlap is 50 mm. We have mounted this reader at a distance of 30 mm to the floor. At this distance, the detection area of the reader has a circular shape with a diameter of 90 mm. The orientation of the reader has only a small impact on the detection area.

The second reader is a “KTS SRR1356 ShortRange HF Reader” with an external antenna with the rectangular shape 80 mm × 80 mm (*reader 2*). We have mounted this reader at a distance of 15 mm to the floor. At this distance, the detection area of the reader has also a circular shape but with a larger diameter of 200 mm

The RFID transponders in the floor are placed in a regular grid of 250 mm. Thus, with both readers at most one RFID transponder can be detected at any moment. Both readers are mounted in the center of the vehicles frame ( ${}^A\mathbf{T}_V = \mathbf{I}$ ). Thus, the heading of the vehicle has no impact on the reading region  $\mathcal{R}_i$ . In case of our experimental setup, the border of the detection area can be modeled

$$g(\mathbf{h}(\mathbf{x}_k, \mathbf{t}_i, \mathbf{v}_k)) = \sqrt{(x_k - x_i + v_x)^2 + (y_k - y_i + v_y)^2} - r \quad (14)$$

for both readers, where  $x_i, y_i$  is the position of  $T_i$  in world frame,  $x_k, y_k$  is the position of the vehicle (center of the vehicle frame),  $r$  is the radius of the detection area and  $\mathbf{v}_k = (v_x, v_y)^\top$  is the measurement noise. In order to apply the measurement update  $g(\mathbf{x}_k, \mathbf{v}_k)$  to an EKF its Jacobians are needed:

$$\mathbf{G}_k = \frac{\partial g}{\partial \mathbf{x}}(\hat{\mathbf{x}}_k, \mathbf{t}_i, \mathbf{0}) = \begin{pmatrix} \frac{x_k - x_i}{\sqrt{(x_k - x_i)^2 + (y_k - y_i)^2}} & \frac{y_k - y_i}{\sqrt{(x_k - x_i)^2 + (y_k - y_i)^2}} & 0 \end{pmatrix}, \quad (15)$$

and

$$\mathbf{V}_{k,i} = \frac{\partial g_i}{\partial \mathbf{v}}(\hat{\mathbf{x}}_k, \mathbf{t}_i, \mathbf{0}) = \mathbf{G}_{k,i} \quad (16)$$

### C. Omnidirectional Transport Vehicle

This section summarizes the probabilistic motion model of a Mecanum based vehicle we have developed in [4] and [10]. An omnidirectional vehicle is able to move in any direction and to rotate around its z-axis at the same time. Our vehicle is equipped with Mecanum wheels, which provide three degrees of freedom. An example of a Mecanum based transport vehicle is shown in Fig. 5. The movements of the vehicle are corrupted



Figure 5. Omnidirectional vehicle with Mecanum wheels

by disturbances caused by mechanical inaccuracies such as unequal floor contact, wheel slippage and inaccuracies in the speed control of the wheels that lead to coupling errors. This disturbances will be treated as process noise. Experiments with an omnidirectional vehicle show, that the noise is mainly caused by slippage of the Mecanum wheels. Since the slippage of the wheels depends on the rotational speed of the free spinning rollers, the uncertainty depends on the direction of the movement in the vehicle frame. Therefore, it is assumed that the movements of the vehicle in the vehicle frame are corrupted by independent noise  $\epsilon_i$ :

$$\Delta \hat{x}_R = \Delta x_R + \epsilon_x, \quad \Delta \hat{y}_R = \Delta y_R + \epsilon_y, \quad \Delta \hat{\theta}_R = \Delta \theta_R + \epsilon_\theta \quad (17)$$

Furthermore it is assumed, that the noise  $\epsilon_i$  is normally distributed with zero mean  $\epsilon_i = \mathcal{N}(0, \sigma_i^2)$ . The standard deviation  $\sigma_i$  is proportional to the displacement in the vehicle frame and changes in the coupling error  $\Delta \varphi_e$ :

$$\begin{pmatrix} \sigma_x \\ \sigma_y \\ \sigma_\theta \end{pmatrix} = \begin{pmatrix} \alpha_x^x & \alpha_x^y & \alpha_x^\theta & \alpha_x^e \\ \alpha_y^x & \alpha_y^y & \alpha_y^\theta & \alpha_y^e \\ \alpha_\theta^x & \alpha_\theta^y & \alpha_\theta^\theta & \alpha_\theta^e \end{pmatrix} \cdot \begin{pmatrix} \Delta x_R \\ \Delta y_R \\ \Delta \theta_R \\ \Delta \varphi_e \end{pmatrix} \quad (18)$$

The parameters  $\alpha_i^j$  are vehicle-specific constants, which can be identified by experiments. With the additional noise, the motion model can be described as follows:

$$\mathbf{x}_k = \mathbf{f}(\mathbf{x}_{k-1}, \mathbf{u}_k, \mathbf{w}_k), \quad \text{with } \mathbf{x}_k = \begin{pmatrix} x_k \\ y_k \\ \theta_k \end{pmatrix}, \quad (19)$$

$$\mathbf{u}_k = \begin{pmatrix} \Delta x_R \\ \Delta y_R \\ \Delta \theta_R \\ \Delta \varphi_e \end{pmatrix}, \quad \mathbf{w}_k = \begin{pmatrix} \epsilon_x \\ \epsilon_y \\ \epsilon_\theta \end{pmatrix}$$

where  $\mathbf{u}_k$  is obtained by odometry using wheel encoder measurements (see [10]).

$$\begin{aligned} x_k &= x_{k-1} + (\Delta x_R + \epsilon_x) \cos\left(\theta_{k-1} + \frac{\Delta \theta + \epsilon_\theta}{2}\right) \\ &\quad - (\Delta y_R + \epsilon_y) \sin\left(\theta_{k-1} + \frac{\Delta \theta + \epsilon_\theta}{2}\right) \\ y_k &= y_{k-1} + (\Delta x_R + \epsilon_x) \sin\left(\theta_{k-1} + \frac{\Delta \theta + \epsilon_\theta}{2}\right) \\ &\quad + (\Delta y_R + \epsilon_y) \cos\left(\theta_{k-1} + \frac{\Delta \theta + \epsilon_\theta}{2}\right) \\ \theta_k &= \theta_{k-1} + \Delta \theta + \epsilon_\theta \end{aligned} \quad (20)$$

In the prediction step of the EKF, the estimated pose of the vehicle

$$\hat{\mathbf{x}}_k = \mathbf{f}(\hat{\mathbf{x}}_{k-1}, \mathbf{u}_k, \mathbf{0}) \quad (21)$$

and the covariance of the pose

$$P_k = \Phi_k P_{k-1} \Phi_k^T + W_k Q_k W_k^T, \quad (22)$$

can be calculated based on  $f(\cdot)$  and its Jacobians  $\Phi_k$  and  $W_k$ :

$$\Phi_k = \frac{\partial f}{\partial \mathbf{x}}(\hat{\mathbf{x}}_k, \mathbf{u}_k, \mathbf{0}) \quad \text{and} \quad W_k = \frac{\partial f}{\partial \mathbf{w}}(\hat{\mathbf{x}}_k, \mathbf{u}_k, \mathbf{0}) \quad (23)$$

The process covariance matrix

$$Q_k = \begin{pmatrix} \sigma_x^2 & 0 & 0 \\ 0 & \sigma_y^2 & 0 \\ 0 & 0 & \sigma_\theta^2 \end{pmatrix} \quad (24)$$

can be calculated using (18).

## VI. EXPERIMENTAL RESULTS

We have made several experiments with one of our omnidirectional vehicles and two different RFID readers in our lab on the NaviFloor<sup>®</sup> installation. The measurements of the RFID reader and the wheel encoders are stored in a file and evaluated off-line with Matlab. Fig. 6 shows results from one of our experiments with *reader 1*. The vehicle moves a square path 2 m  $\times$  2 m several times. The heading is constant during the whole movement ( $\theta = -90^\circ$ ). The path of the vehicle is controlled by odometry and gyroscope. The sample time of odometry is 3 ms and the sample time of the RFID reader is 20 ms. Global localization of the vehicle is realized as described in Sec. IV-D. The Pose estimation is started after the second RFID tag is detected. In Fig. 6 RFID tags that are detected by the vehicle are shown as black circles. Since the antenna in mounted in the center of the vehicle frame and the shape of the detection area is circular, the printed circles are the projection of the detection region  $\mathcal{R}_i$  onto the working plane. The path of the vehicle is planned straight over the grid of the transponders. Owing to the small detection area and deviations from the planned path not all transponders are detected. The results of the experiments with *reader 1* show, that only comparable few transponders are detected while traveling a relative long distance. The evaluated filters provide a similar accuracy, a precise benchmark is difficult, since the performances of the filters depend highly on the number of detected transponders and therefore on the exact path. The small detection area of *reader 1* requires a path that is aligned to the tag grid, which restricts free vehicle navigation.

In order to work out the differences of the three filters some experiments with *reader 2* are performed that provides a larger detection area. Fig. 7 shows the results of one experiment with *reader 2*. The vehicle moves a rectangle path 1.5 m  $\times$  3 m in clockwise direction with constant heading ( $\theta = 100^\circ$ ). The path is transverse to the grid with an angle of  $10^\circ$ . The path starts and ends near tag position ( $x = 1750$  mm,  $y = 4500$  mm). All estimators are started after detecting the second tag (1750 mm, 4750 mm) (see Sec. IV-D). Hence, after global localization, the estimated heading is parallel to the grid ( $\hat{\theta} = 90^\circ$ ). Since odometry (magenta curve) is performed without measurement update, its position estimate differs much from real path (black curve). After detecting additional transponders, all filters correct the estimated heading and therefore the direction of movement. The blue curve in Fig. 7 shows, that the PF needs the least way length to correct the misalignment. After detecting the fifth transponder, both KFs corrects the pose estimate and follow

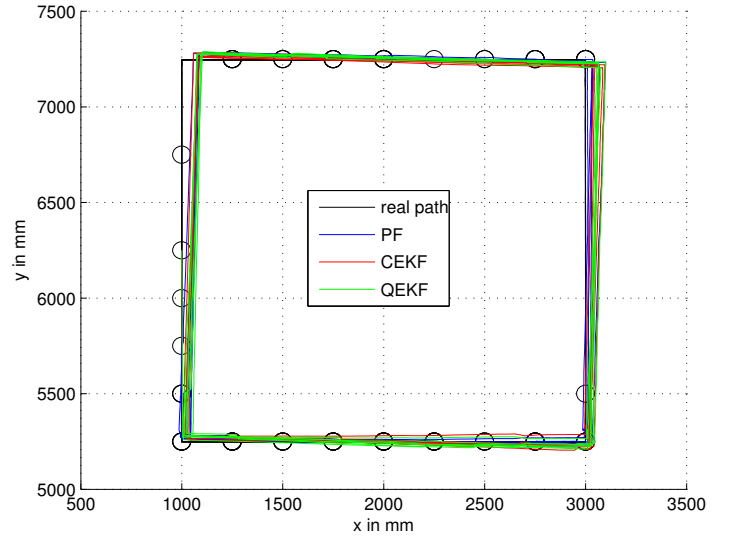


Figure 6. Experimental results with *reader 1*

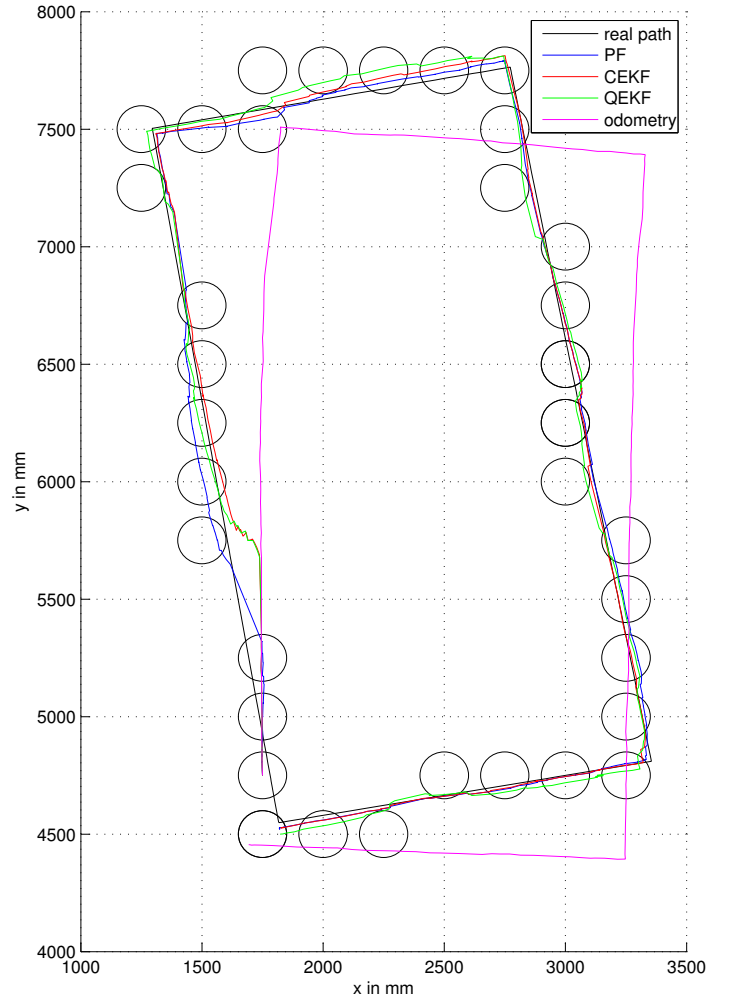


Figure 7. Experimental results with *reader 2*

the real path. The Quantized EKF (QEKF, green curve) tends to force the position estimate into direction of the center of detected transponders. The Constrained EKF (CEKF, red cure)

is able to follow the real path with a smaller deviation than the QEKF. Table I compares the root mean square error (RMSE) of the described filters. The accuracy of the proposed Constrained

Table I. QUANTITATIVE RESULTS WITH *reader 2*

algorithm	odometry	QEKF	CEKF	PF100	PF1000
RMSE in mm	380.5	39.4	29.5	~ 70	~ 30
runtime in ms	0.08	0.27	0.29	8.6	85.4

EKF is similar to a PF with high particle count (1000 particles). A PF with a low particle count (100 particles) has a much lower accuracy than both KF variants. Owing to the particle sampling with random numbers, the RMSE for both PFs differ with every run. Further experiments with *reader 2* confirm this accuracy of the evaluated filters. The CEKF outperforms the QEKF in most cases and provides a similar performance than a PF with high particle count.

Table I compares the duration for one motion plus measurement update of the filters. The durations are measured with Matlab R2014b on a PC with Intel Core i7-2600 CPU 3.40 GHz. The measured durations show that a PF with high particle count is not able to run in real time even on a high speed PC.

## VII. CONCLUSIONS

In this paper, we have presented a novel localization algorithm based on Constrained Kalman filtering that fuses sensory data from wheel encoders with RFID readings. The RFID readings are assumed as noisy constraints of the vehicle's pose. This assumption considers the binary nature of floor-installed HF RFID transponders. The application of the proposed algorithm is possible for any RFID equipment where the border of the detection area can be described by a nonlinear function. The localization accuracy of the Constrained EKF is similar to a PF but with much less computational expense. The accuracy of the localization method is sufficient for most industrial applications. In order to allow a free navigation over the tag grid, the size of the detection area of the reader antenna should be sufficient large enough compared to the grid size.

The localization concept is suitable for small and inexpensive robotic vehicles, since the vehicles must be equipped with an inexpensive and small HF RFID reader only. Compared to localization using laser range finders as position sensor, a HF RFID reader is more than 10 times cheaper. Compared to localization using optical or inductive guidance, localization using a grid of floor-installed transponders is much more flexible. The installation of the RFID infrastructure causes the highest expense for this localization method, but since passive RFID technology is used, the infrastructure is free of maintenance costs.

## REFERENCES

- [1] J.-H. Kämper, A. Stasch, and A. Hahn, "A fully-automated manufacturing environment realized through a flexible in house logistic system with smart transportation infrastructure," in *Proceedings of the 2014 ICAM International Conference on Advanced and Agile Manufacturing*, Oakland University, Rochester, MI 48309, USA, 2014.
- [2] A. Nettstätter, J. R. Nopper, C. Prasse, and M. t. Hompel, "The internet of things in logistics," in *Smart Objects: Systems, Technologies and Applications (RFID Sys Tech)*, 2010 European Workshop on, June 2010, pp. 1-8.

- [3] T. Kirks, J. Stenzel, A. Kamagaew, and M. ten Hompel, "Cellular transport vehicles for flexible and changeable facility logistics systems," *Logistics Journal*, vol. 2192, no. 9084, p. 1, 2012.
- [4] C. Röhrig, D. Heß, C. Kirsch, and F. Künemund, "Localization of an Omnidirectional Transport Robot Using IEEE 802.15.4a Ranging and Laser Range Finder," in *Proceedings of the 2010 IEEE/RSJ International Conference on Intelligent Robots and Systems (IROS 2010)*, Taipei, Taiwan, Oct. 2010, pp. 3798-3803.
- [5] E. Guizzo, "Three Engineers, Hundreds of Robots, one Warehouse," *IEEE Spectrum*, vol. 7, pp. 27-34, 2008.
- [6] G. Liu, W. Yu, and Y. Liu, "Resource management with RFID technology in automatic warehouse system," in *Intelligent Robots and Systems, 2006 IEEE/RSJ International Conference on*, 2006, pp. 3706-3711.
- [7] T. Kämpke, B. Kluge, and M. Strobel, "Exploiting RFID capabilities onboard a service robot platform," in *Towards Service Robots for Everyday Environments*, ser. Springer Tracts in Advanced Robotics, E. Prassler, M. Zöllner, R. Bischoff, W. Burgard, R. Haschke, M. Hägele, G. Lawitzky, B. Nebel, P. Plöger, and U. Reiser, Eds. Springer Berlin Heidelberg, 2012, vol. 76, pp. 215-225.
- [8] Götting KG, "Introduction transponder positioning," <http://www.goetting-agv.com/components/transponder/introduction>.
- [9] M. Baum, B. Niemann, and L. Overmeyer, "Passive 13.56 MHz RFID transponders for vehicle navigation and lane guidance," in *Proceedings of the 1st International EUR AS IP Workshop on RFID Technology*, 2007, pp. 83-86.
- [10] C. Röhrig, A. Heller, D. Heß, and F. Künemund, "Global localization and position tracking of automatic guided vehicles using passive RFID technology," in *Proceedings of the joint 45th International Symposium on Robotics (ISR 2014) and the 8th German Conference on Robotics (ROBOTIK 2014)*, Munich, Germany, Jun. 2014.
- [11] K. Kodaka, H. Niwa, Y. Sakamoto, M. Otake, Y. Kanemori, and S. Sugano, "Pose estimation of a mobile robot on a lattice of RFID tags," in *Intelligent Robots and Systems, 2008. IROS 2008. IEEE/RSJ International Conference on*, 2008, pp. 1385-1390.
- [12] B.-S. Choi, J.-W. Lee, J.-J. Lee, and K.-T. Park, "A hierarchical algorithm for indoor mobile robot localization using RFID sensor fusion," *Industrial Electronics, IEEE Transactions on*, vol. 58, no. 6, pp. 2226-2235, 2011.
- [13] J. Lee, Y. Park, D. Kim, M. Choi, T. Goh, and S.-W. Kim, "An efficient localization method using RFID tag floor localization and dead reckoning," in *Control, Automation and Systems (ICCAS), 2012 12th International Conference on*, 2012, pp. 1452-1456.
- [14] E. DiGiampaolo and F. Martinelli, "A passive UHF-RFID system for the localization of an indoor autonomous vehicle," *Industrial Electronics, IEEE Transactions on*, vol. 59, no. 10, pp. 3961-3970, 2012.
- [15] M. Boccadoro, F. Martinelli, and S. Pagnottelli, "Constrained and quantized kalman filtering for an RFID robot localization problem," *Autonomous Robots*, vol. 29, no. 3-4, pp. 235-251, 2010.
- [16] A. Levratti, M. Bonaiuti, C. Secchi, and C. Fantuzzi, "An inertial/RFID based localization method for autonomous lawnmowers," in *Proceedings of the 10th IFAC Symposium on Robot Control, IFAC SYROCO 2012*, Dubrovnik, Croatia, Sep. 2012, pp. 145-150.
- [17] D. Simon, "Kalman filtering with state constraints: a survey of linear and nonlinear algorithms," *Control Theory Applications, IET*, vol. 4, no. 8, pp. 1303-1318, August 2010.
- [18] V. Sircoulomb, G. Hoblos, H. Chafouk, and J. Ragot, "State estimation under nonlinear state inequality constraints. a tracking application," in *Control and Automation, 2008 16th Mediterranean Conference on*, June 2008, pp. 1669-1674.
- [19] R. E. Curry, *Estimation and Control with Quantized Measurements*. MIT Press Cambridge, 1970.
- [20] A. Steinhage and C. Lauterbach, "SensFloor<sup>®</sup> and NaviFloor<sup>®</sup>: Large-area sensor systems beneath your feet," in *Handbook of Research on Ambient Intelligence and Smart Environments: Trends and Perspectives*, N. Chong and F. Mastrogianni, Eds. Hershey, PA: Information Science Reference, 2011, pp. 41-55.